

Cite this article as: Wang Ding, Sun Yunan, Xue Zhiguo, et al. Preparation and Properties of Large-Size Titanium-Steel Composite Plates[J]. Rare Metal Materials and Engineering, 2023, 52(11): 3723-3729. DOI: 10.12442/j.issn.1002-185X.20230180.

ARTICLE

Preparation and Properties of Large-Size Titanium-Steel Composite Plates

Wang Ding¹, Sun Yunan¹, Xue Zhiguo¹, Zhang Penghui¹, Wu Jiangtao^{1,2}, Fan Keshe^{1,2}, Huang Xingli¹

¹Xi'an Tianli Clad Metal Materials Co., Ltd, Xi'an 710201, China; ²Shaanxi Engineering Research Center of Metal Clad Plate, Xi'an 710201, China

Abstract: Titanium-steel composite plates with large sizes of 4260 mm×4260 mm×(6.5+32) mm were prepared by explosive welding technique. Ultrasonic nondestructive testing, phased-array waveform microscopy, optical microscope, and scanning electron microscope were used to analyze the mechanical properties and interface morphologies of the composite plates. Results show that when the detonation velocity, density, explosive height, and stand-off distance are 2200–2270 m/s, 0.80–0.82 g/cm³, 45.0–46.0 mm, and 8.0–11.0 mm, respectively, the mechanical properties of the prepared plates can satisfy ASTM B898-2020 technical requirements. The interface waveform presents a typical periodic combination morphology and the interface is clear and uniform. A small amount of solidified melt exists in the vortex area of waveform. The ratio of amplitude to wavelength ranges from 0.15 to 0.25, and the optimal shear strength can be achieved when the ratio is approximately 0.20. This research provides preparation technique for the large-size titanium-steel composite plates and theoretical guidance for the subsequent optimization of the explosive welding process of composite plants.

Key words: large-size titanium-steel composite plate; phased array; interface microstructure; mechanical properties; amplitude ratio

To prepare functional materials with different physical, chemical, and mechanical properties, more and more attention has been paid on the special processes^[1–4]. As an important structural connection method, the explosive welding technique has the characteristics of diffusion welding, melt welding, and pressure welding. The explosive welding technique can possess different materials with controllable sizes, superior interface bonding strength, and reprocessing performance^[5–7]. Therefore, it is widely used in aerospace, nuclear power, atomic energy, and other fields.

Titanium has the characteristics of high strength and excellent corrosion resistance at different temperatures. To save titanium resources, reduce equipment cost, improve equipment quality, and shorten the maintenance time, titanium-steel composite plates are widely used in the fields of pure terephthalic acid preparation, oxidation reactors, solvent dehydration towers, and heat exchanger in the modern chemical industry and pressure vessel industry^[8–11]. The

composite materials containing titanium and titanium alloys have high deformation resistance and low impact toughness, therefore being difficult to process^[12]. However, the adiabatic shear line easily appears on the titanium layer after the explosive welding, which restricts the manufacture of large-size composite plates, the optimization of interface quality, and the performance improvement. Fig.1 shows the dynamic change of interface during explosive welding.

The materials, explosives, and interface-forming mechanisms of small plates have been extensively researched^[13–19]. Due to the difference in properties between base and flyer materials, the resultant explosive welding windows are different^[12]. In the actual production preparation, the quality of finished product cannot satisfy the requirements based on explosive welding theory. The ripple of the bonding interface formed by explosive welding can directly affect the final quality of products, which is affected by many factors^[20–23]. With increasing the size of composite plates, the uniformity of

Received date: April 04, 2023

Foundation item: Shaanxi Provincial Key Research and Development Program Project Fund (2018ZDCXL-G-3)

Corresponding author: Huang Xingli, Master, Senior Engineer, Xi'an Tianli Clad Metal Materials Co., Ltd, Xi'an 710201, P. R. China, Tel: 0086-29-86968325, E-mail: 15339276169@126.com

Copyright © 2023, Northwest Institute for Nonferrous Metal Research. Published by Science Press. All rights reserved.

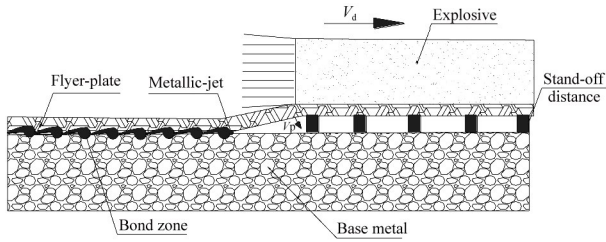


Fig.1 Dynamic change of interface during explosive welding

explosive composite, and the stability of detonation wave in production, longer duration is required to exhaust air at a fixed detonation velocity during the manufacture process. The more difficult the air exhaustion, the more difficult the process control. Therefore, it is critical to study the interface characteristics of titanium-carbon steel composite plates in large specifications. The theory formula of detonation pressure is $P = \rho_0(\rho - \rho_0)/\rho V_d^2$ (P is detonation pressure; V_d is the detonation velocity; ρ_0 is the initial density of explosives; ρ is the density of explosive products). During the explosion reaction, the superposition of detonation wave and explosive products result in the increase in pressure as well as plate width and the decrease in stability. Thus, the detonation velocity and detonation pressure are the key factors to prepare high-quality composite plates^[24-25].

1 Experiment

Industrial titanium B265 Gr. 1 (namely Gr. 1) and carbon steel A516 Gr. 70 (namely Gr. 70) were selected as the flyer plate and base plate with the size of 4550 mm×4550 mm×(6.5+32) mm. The chemical composition and mechanical properties of titanium plate and carbon steel plate are shown in Table 1– Table 3.

In the process parameter design, the long-distance detonation wave and the low bonding strength during the explosive welding should be comprehensively considered, thereby resulting in low detonation energy and difficulties in air exhaustion. These two factors can be affected by gap height, explosive thickness, explosive burst speed, explosive

density, and other process parameters. Additionally, the interface over-melting phenomenon should be avoided, because the high energy may cause tear at the composite plate edge. Fig. 2 shows the device of explosive welding at operation site.

According to the preparation characteristics of large-size titanium-steel composite plate, the parallel installation conditions in the explosive welding process are $V_p = 2\sin(\Phi/2)$ and $V_p = V_d$. The detonator was placed in the geometric center and the explosives were laid evenly on the flyer plate. Then, the minimum velocity V_m of the collision point should satisfy the relationship, as follows:

$$V_m = \left| \frac{2Re(H_1 + H_2)}{\rho_1 + \rho_2} \right|^{1/2} \quad (1)$$

where Reynolds number Re is 8.9; H_1 and H_2 are the Vickers hardness of cladding and base plates, respectively; ρ_1 and ρ_2 are the densities of cladding and base plates, respectively. To ensure the formation of stable reentry jet, V_p should be less than the sound volume velocity of cladding material (V_s), as follows:

$$V_s = \left| \frac{E}{3(1 - 2\nu)\rho} \right|^{1/2} \quad (2)$$

where E is the elastic modulus of titanium plate, ρ is the material density, and ν is Poisson's ratio.

Therefore, the moving speed of the collision point should satisfy $V_m < V_p < V_s$. Based on the calculated V_m values, the collision rate can be expressed, as follows:

$$\begin{aligned} V_p &= V_m + 200 & V_m < 2000 \text{ m/s} \\ V_p &= V_m + 100 & 2000 < V_m < 2500 \text{ m/s} \\ V_p &= V_m + 50 & V_m > 2500 \text{ m/s} \end{aligned} \quad (3)$$

The explosive velocity is a key parameter in theoretical calculation. The calculated explosive velocity is $V_m = 2077$ m/s. Therefore, the optimal theoretical detonation velocity is 2177 m/s. In this research, the detonation velocity is the same as the moving speed of the interface collision point of titanium-steel composite plate. To ensure the lower limit of weldability window requirements of the detonation velocity, the velocity should be controlled within 2200–2270 m/s. Additionally, by adding diluents into the industrial powdered ammonium nitrate explosives, the explosives can satisfy the requirements and have a stable physical and chemical state.

In the preparation process, the contact surfaces of the base plate and cladding plate should be polished until they are flat, smooth, and clean. The average roughness of the base and cladding plate surfaces R_a should be less than 1.6 μm . Before the explosive welding, the surface is evenly coated with a butter layer to prevent the surface burning caused by high pressure and high temperature. Large-size titanium plates have

Table 1 Chemical composition of Gr.1 plate (wt%)

Fe	C	N	O	H	Ti
0.021	0.004	0.003	0.003	0.0009	Bal.

Table 2 Chemical composition of Gr.70 plate (wt%)

Cr	Mn	Ni	P	Si	Ti	C	Fe
0.084	1.48	0.17	0.017	0.32	0.013	0.169	Bal.

Table 3 Mechanical properties of Gr.1 plate and Gr.70 plate

Plate	Tensile strength/ MPa	Yield strength/ MPa	Elongation/ %	Density/kg·m ⁻³	Vickers hardness, HV/ ×9.8 MPa	Elastic modulus/ GPa	Poisson's ratio, ν
Gr.1	304	275	44	4510	139	116	0.34
Gr.70	567	336	35	7830	160	200	0.33

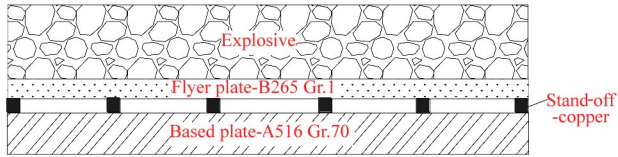


Fig.2 Device of explosive welding at operation site

inferior flatness and uniformity, which results in bending and subsidence phenomena. The decrease in spacing reduces the acceleration time of cladding plate and also decreases the impact velocity. Jet cannot be generated unless the impact velocity of the cladding plate reaches the critical value, which is obtained by the theoretical calculation and practical production^[25]. Six processes of different explosive and support heights for areas A and B were designed, as shown in Fig. 3. After the detonation tube was ignited, the explosion velocity increased and gradually reached the stability within an area of 1800 mm in radius in a very short time. Fig. 3 shows the schematic diagram of explosive welding site, and Table 4 presents the explosive parameters of explosive welding site.

After explosive welding, the ultrasonic nondestructive test, phased array interface imaging, interface ripple metallography, and shear strength test were conducted for six composite plates. The mechanical properties of annealed materials were tested. The interface hardness of the explosive and annealed states was measured, and the typical interface structure was observed by the scanning electron microscope (SEM). Anyscan-31 ultrasonic flaw detector was used for the nondestructive testing of composite plates, and an Olympus flaw detector was used for the interface imaging. The standard

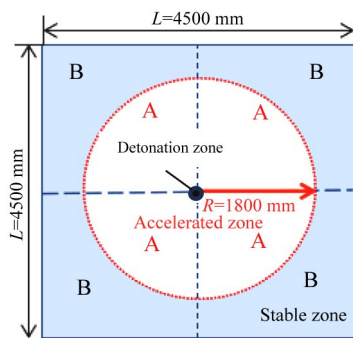


Fig.3 Schematic diagram of explosive welding site

of ASTM B898-2020 Class A^[26] was employed to evaluate the composite plate. Tensile test was conducted according to ASTM E8/E8M-17A standard by the electronic universal testing machine (CMT5105). The impact test was conducted by MIRIE-F1432 750J pendulum impact testing machine based on ASTM E23-2017 standard. The specimens for shear strength tests were pre-treated according to ASTM B898-2020 standard. The microstructures were analyzed by optical microscope (OM, MIRIE-F2573), the Vickers hardness tester was MIRIE-F1433, and the interface structures were analyzed by VEGA 3 XMU tungsten filament SEM.

2 Results and Discussion

2.1 Ultrasonic nondestructive test

For ultrasonic nondestructive testing of six composite plates, the coupling agent conditions were 2.5 P, single probes ($\Phi 20$ mm), and water. The direct contact method was used for ultrasonic testing of the whole plate through the diffraction time difference method, which is in accordance with the requirements of ASTM B898-2020 Class A. The minimum overall sound bond area should be 99% of the total area. Except for the detonator area within the area of $\Phi 25$ mm on the composite plate, the bonding rate of effective areas reached 100%, and the result of ultrasonic nondestructive testing could satisfy the technical requirements.

During the phased array interface imaging of composite plate, 10L128 probe was used. Fig. 4 shows the phased array imaging morphology of bonding interface of titanium-steel composite plate. It can be found that the bonding interface of the composite plate presents the typical wave-like bonding with a uniform ripple.

2.2 Interface morphology characteristics

Fig. 5 show OM morphologies of interface structures of titanium-steel composite plates after processing with different parameters. It can be found that under the impact of detonation velocity, large plastic deformation occurs in the cladding layer, base layer, and bonding interface. The bonding interface of titanium-steel composite plate presents a typical wave-like bonding, which repeats periodically along the direction of detonation wave propagation at the titanium-steel interface. The waveform has vortex characteristics. There is no obvious melting phenomenon. Only a small number of melting blocks exist in the vortex region.

The melt originates from the bonding interface and the

Table 4 Explosive parameters of explosive welding sites

Process No.	Detonation velocity/ $m \cdot s^{-1}$	Density/ $g \cdot cm^{-3}$	Explosive height/mm	Distance of stand-off/mm	
				Area A	Area B
1	2200–2230	0.80–0.81	45.0–46.0	8.0	8.0
2	2200–2230	0.80–0.81	45.0–46.0	8.0	9.0
3	2200–2230	0.80–0.81	45.0–46.0	9.0	9.0
4	2230–2270	0.81–0.82	41.0–42.0	9.0	10.0
5	2230–2270	0.81–0.82	41.0–42.0	10.0	10.0
6	2230–2270	0.81–0.82	41.0–42.0	10.0	11.0

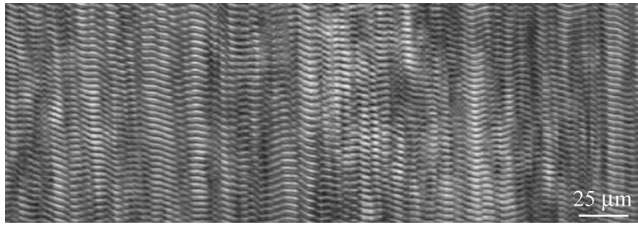


Fig.4 Phased array imaging morphology of bonding interface of titanium-steel composite plate

inside vortex. Based on the mechanism of explosive welding formation, it is necessary to produce metal jets for the successful implementation of explosive welding. Therefore, the melting and partial melting phenomena are inevitable. When the collision speed is low, the material softening and explosive welding cannot be achieved. When the interface temperature is too high, too much melt is generated and a large number of holes or a large amount of melt exists in the bonding interface. The wave amplitude and wavelength of the interface of different composite plates were measured three

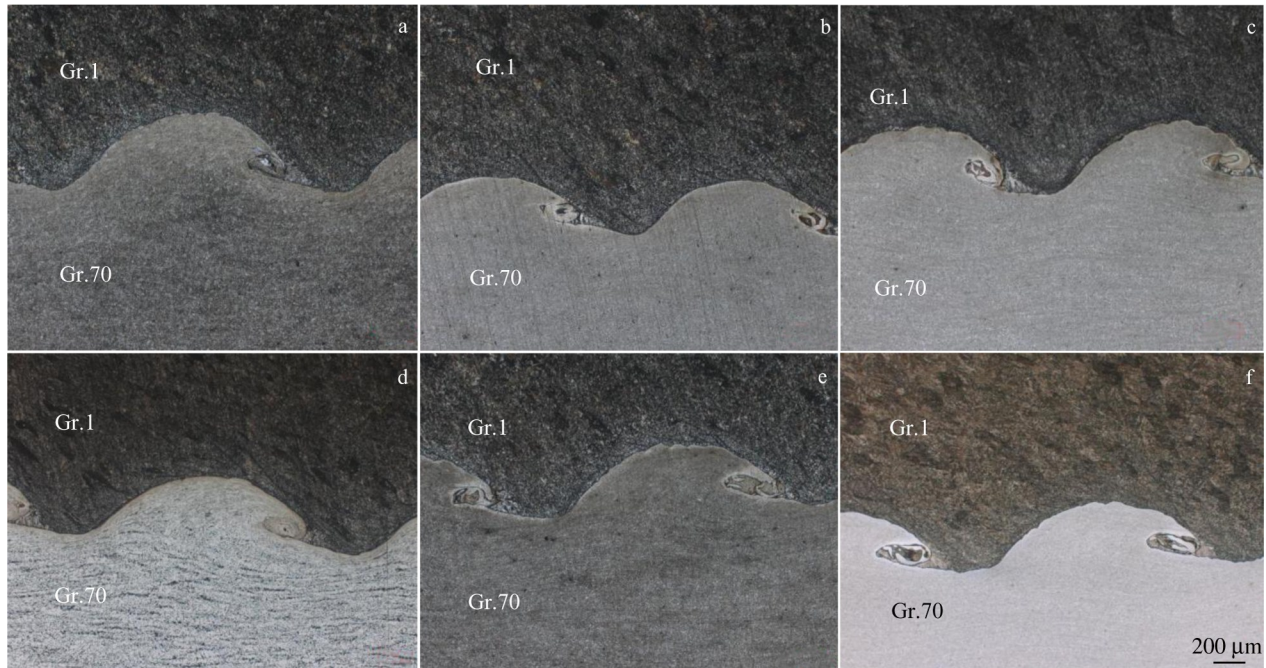


Fig.5 OM morphologies of interface structures of titanium-steel composite plates after processing with different parameters: (a) process 1; (b) process 2; (c) process 3; (d) process 4; (e) process 5; (f) process 6

times to obtain the average value by metallographic test. Table 5 shows the calculation results of the wave amplitude ratio R (the ratio of wave amplitude to wavelength) of the six plates, which are all between 0.15 and 0.25.

2.3 Mechanical properties

2.3.1 Tensile and impact results

After heat-treatment of the titanium-steel composite plates, tensile and impact tests were conducted. The testing position was at the middle of the side line of the composite plates. Table 6 shows the results of the tensile tests at room temperature and impact tests at $-46\text{ }^{\circ}\text{C}$, which satisfy the requirements of ASTM B898-2020 standard. Therefore, for the preparation of large-size titanium-steel composite plates, the

detonation velocity, density, explosive height, and distance of stand-off should be 2200–2270 m/s, 0.80–0.82 g/cm³, 45.0–46.0 mm, and 8.0–11.0 mm, respectively. The resultant product has excellent mechanical properties, which satisfy the requirements of ASTM B898-2020 standard.

2.3.2 Shear strength

The shear tests were conducted at the plate corner, which was away from the end of the plate detonation point. Each plate was subjected to three shear tests. The results of shear strength are shown in Table 7. The results range from 170 MPa to 240 MPa, with an average value of 211 MPa, which

Table 5 Wave amplitude ratio (R) of different composite plates

Process	1	2	3	4	5	6
1st measurement	0.188	0.194	0.156	0.196	0.226	0.230
2nd measurement	0.186	0.191	0.156	0.190	0.221	0.241
3rd measurement	0.187	0.196	0.161	0.194	0.224	0.240

Table 6 Experiment results of tensile tests at room temperature and impact tests at $-46\text{ }^{\circ}\text{C}$

Batch	Tensile strength/MPa	Yield strength/MPa	Elongation /%	Impact energy/J
1	534	358	33.5	128, 132, 148
2	537	350	31.0	183, 169, 179
3	526	346	31.0	128, 132, 148

Table 7 Experiment results of shear strength of different composite plates (MPa)

Process	1	2	3	4	5	6
1st measurement	211	217	176	233	214	213
2nd measurement	208	214	177	237	212	212
3rd measurement	211	217	178	238	216	214

are all higher than the required shear strength (137.9 MPa) in ASTM B898-2020 for composite plates. The amplitude ratio results are in good agreement with the shear strength results, and their relationship is shown in Fig.6.

2.3.3 Interface Hardness

Fig. 7 presents the Vickers hardness results of both sides of the interface of the explosive-welded and annealed composite plates at the bonding zone. It can be seen that the smaller the distance between the titanium plate and steel plate, the more obvious the deformation. The hardening effect is obvious. Additionally, the cooling rate during the explosive welding is extremely high. Due to the local high temperature and high pressure, the carbon elements from the titanium plate and steel plate cannot diffuse. Therefore, the supersaturated solid solutions or hard and brittle intermetallic compounds are formed, resulting in high hardness of the interface.

After low-temperature annealing treatment, the hardening

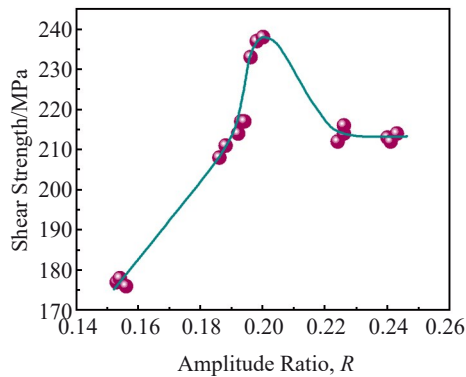


Fig.6 Relationship between shear strength and amplitude ratio R of different composite plates

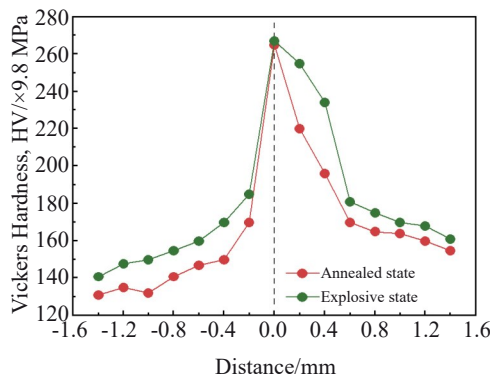


Fig.7 Vickers hardness HV of explosive-welded and annealed titanium-steel composite plates

effect induced by explosive welding is released. At the place with the same distance from the interface, the hardness of the annealed composite plate is significantly less than that of the explosive one. The change near the interface deformation zone is particularly obvious. The farther the distance away from the interface, the more stable the hardness and the more uniform the hardness distribution. Thus, the plastic deformation of the composite plate is enhanced and the workability is improved. In conclusion, after the explosive welding, the maximum hardness (HV) of composite plate is 2548–2646 MPa, and the hardening effect is obvious. After annealing treatment, the stress and the hardness decrease, whereas the plasticity improves, which is beneficial to the deformation.

2.4 Interface organization characteristics

Fig. 8 shows OM image of interface structure of titanium-steel composite plate after process 4, which is typical and similar to that of other composite plates. On the titanium side, there is no regular deformation near the interface, but a large number of adiabatic shear lines are generated. Under the high-speed impact, plastic deformation starts from the local area of the material. The heat of local plastic deformation cannot be transferred immediately, and the heat accumulation reduces the local yield strength. When the dynamic yield strength is lower than the shear stress generated by the impact load, the instantaneous shear deformation occurs. On the carbon steel side, the closer the distance to the interface, the greater the grain deformation. The original equiaxed crystal along the deformation direction gradually elongates, and the degree of grain elongation is significant. When the deformation is very large, the grains are difficult to distinguish, presenting the shape of fibrous stripes. Fig.9 shows SEM image of interface structure of titanium-steel composite plate after process 4. It can be found that both sides of the titanium plate and steel plate maintain their respective organizational components. The interface formation of the titanium-steel composite plate is mainly dominated by the plastic deformation. The microstructure characteristics of both sides of the titanium-steel composite plate are consistent with the hardness results of the interface.

Through the non-destructive test results, mechanical



Fig.8 OM image of interface structure of titanium-steel composite plate after process 4

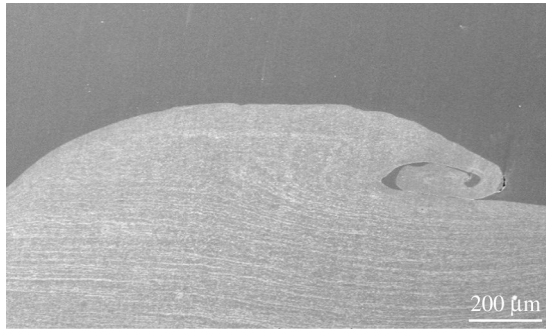


Fig.9 SEM image of interface structure of titanium-steel composite plate after process 4

properties, and interface composition analyses of the composite plates, it can be found that there is no combination for the detonation area with diameter of 25 mm, and the effective areas are well combined. The shear strength, tensile strength, and impact properties of the composite plate can satisfy the requirements of ASTM B898-2020 standard. The interface ripples of the titanium-steel composite plate are uniform. The wave amplitude ratio, namely interface ripple ratio, is between 0.15 and 0.25. With increasing the wave amplitude ratio, the shear strength is increased gradually, then decreased, and finally stabilized. The composite plate after process 4 has the highest shear strength at wave amplitude ratio=0.2. Reducing the explosive height and increasing the edge gap height are beneficial to exhaust air of the explosive welding process. These results all provide guidance for the combination of large-size composite plates by explosive welding process.

3 Conclusions

1) For the preparation of large-size titanium-steel composite plates, the detonation velocity, density, explosive height, and distance of stand-off should be 2200 – 2270 m/s, 0.80 – 0.82 g/cm³, 45.0–46.0 mm, and 8.0–11.0 mm, respectively. The resultant product has excellent mechanical properties, which satisfy the requirements of ASTM B898-2020 standard.

2) After explosive welding, the maximum Vickers hardness (HV) of composite plate is 2548 – 2646 MPa, and the hardening effect is obvious. After annealing treatment, the stress and the hardness decrease, whereas the plasticity improves, which is beneficial to the deformation.

3) The bonding interface presents the typical wave-like bonding, the shear strength is between 170 and 240 MPa, and the wave amplitude ratio is between 0.15 and 0.25. When the detonation velocity, density, explosive height, and distance of stand-off are 2230–2270 m/s, 0.81–0.82 g/cm³, 41.0–42.0 mm, and 9 – 10 mm, respectively, the composite plate has the optimal shear strength at wave amplitude ratio=0.2.

References

- Feng J R, Dai K D Zhou Q et al. *Journal of Physics Condensed Matter*[J], 2019, 31(41): 415 403
- Feng J R, Liu R, Liu K Y et al. *Journal of Applied Physics*[J], 2022, 131(2): 25 903
- Ren B, Tao G, Wen P et al. *International Journal of Refractory Metals and Hard Materials*[J], 2019, 84: 105 005
- Vaidyanathan P V, Ramanathan A. *Journal of Materials Processing Technology*[J], 1992, 32(1–2): 439
- Li Y, Liu C R, Yu H B et al. *Metals*[J], 2017, 7(10): 407
- Zu G, Xi S, Zhang J G. *Rare Metal Materials and Engineering*[J], 2017, 46(4): 906
- Acarer M, B. Gülen B, Findik F. *Journal of Materials Science*[J], 2004, 39(21):6457
- Kahraman N, BehetGülen, Findik F. *Journal of Materials Processing Technology*[J], 2005, 169(2): 127
- Manikandan P, Hokamoto K, Fujita M et al. *Journal of Materials Processing Technology*[J], 2008, 195(1–3): 232
- Gloc M, Wachowski M, Plocinski T et al. *Journal of Alloys and Compounds*[J], 2016, 671: 446
- Borchers C, Lenz M, Deutges M et al. *Materials and Design*[J], 2015, 89(8): 369
- Shi C G, Yang X, Ge Y H et al. *Journal of Iron and Steel Research, International*[J], 2017, 24(8): 852
- Zlobin B S, Kiselev V V, Shtertser A A. *Combustion, Explosion, and Shock Waves*[J], 2022, 58(1): 121
- Zhang Z L, Liu M B. *Journal of Manufacturing Processes*[J], 2019, 41: 208
- Yang M, Xu J F, Ma H H et al. *Composites Part B: Engineering*[J], 2021, 212: 108 685
- Acarer M, Gülenç B, Findik F. *Materials & Design*[J], 2003, 24(8): 659
- Durgutlu A, Okuyucu H, Gulenc B. *Materials and Design*[J], 2008, 29(7): 1480
- Jaramillov D, Inal O T, Szecket A. *Journal of Materials Science*[J], 1987, 22(9): 3143
- Jaramillo D, Szecket A, Inal O T. *Materials Science and Engineering*[J], 1987, 91(87): 217
- Greenberg B A, Ivanov M A, Inozemtsev A V et al. *Metallurgical and Materials Transactions A*[J], 2015, 46: 3569
- Wang Xinyu, Li Xiaojie, Wang Xiaohong et al. *Explosion and Shock Waves*[J], 2014, 34(6): 716 (in Chinese)
- Shi Changgen, Wang Yaohua, Li Zhiquan et al. *Explosive Materials*[J], 2004, 33(5): 25 (in Chinese)
- Reid S R, Sherif N H S. *Journal of Mechanical Engineering Science*[J], 1976, 18(2): 87
- Stivers S W, Wittman R H. *High Energy Rate Fabrication*[M]. Colorado: University of Denver Research Institute, 1975
- An Lichang. *Chinese Journal of Explosives & Propellants*[J], 2003, 26(3): 68 (in Chinese)
- ASTM International. ASTM B898-2020[S], 2020

大规格钛-钢复合板的制备及性能

王 丁¹, 孙雨楠¹, 薛治国¹, 张鹏辉¹, 吴江涛^{1,2}, 樊科社^{1,2}, 黄杏利¹

(1. 西安天力金属复合材料有限公司, 陕西 西安 710201)

(2. 陕西省层状金属复合材料工程研究中心, 陕西 西安 710201)

摘 要: 采用爆炸焊接技术制备尺寸为4260 mm×4260 mm×(6.5+32) mm的钛-钢复合板。采用超声波无损检测、相控阵波形显微镜、金相显微镜和扫描电子显微镜对复合材料板材的力学性能和界面形态进行分析。结果表明, 当爆速、密度、炸药高度和间隔距离分别为2200~2270 m/s、0.80~0.82 g/cm³、45.0~46.0 mm和8.0~11.0 mm时, 制备出的板材各项力学性能满足技术指标ASTM B898-2020。界面的波形为典型波纹状结合, 界面清晰均匀, 波形在漩涡区存在少量熔化, 波幅和波长的比值为0.15~0.25, 且在比值为0.2左右时, 产品的剪切强度最高。本研究为大规格钛-钢复合板的制备提供工艺方法, 并发现大规格钛-钢复合板的界面特点, 为后续优化复合板爆炸焊接工艺提供理论指导。

关键词: 大规格钛-钢复合板; 相控阵; 界面形貌; 力学性能; 波幅比

作者简介: 王 丁, 男, 1991年生, 硕士, 工程师, 西安天力金属复合材料股份有限公司, 陕西 西安 710201, 电话: 029-86968325, E-mail: w15209277694@163.com